Biochimica et Biophysica Acta 1817 (2012) 650–657

Contents lists available at SciVerse ScienceDirect

Biochimica et Biophysica Acta

journal homepage: www.elsevier.com/locate/bbabio

Review

Proton transfer in ba_3 cytochrome *c* oxidase from *Thermus thermophilus* ☆

Christoph von Ballmoos [a], Pia Ädelroth [a], Robert B. Gennis [b], Peter Brzezinski [a,*]

[a] Department of Biochemistry and Biophysics, The Arrhenius Laboratories for Natural Sciences, Stockholm University, SE-106 91 Stockholm, Sweden
[b] Department of Biochemistry, University of Illinois, Urbana, IL 61801, USA

ARTICLE INFO

Article history:
Received 29 September 2011
Received in revised form 15 November 2011
Accepted 16 November 2011
Available online 7 December 2011

Keywords:
Respiratory oxidase
Electron transfer
Energy conservation
Electrochemical gradient
Kinetics
Membrane protein

ABSTRACT

The respiratory heme-copper oxidases catalyze reduction of O_2 to H_2O, linking this process to transmembrane proton pumping. These oxidases have been classified according to the architecture, location and number of proton pathways. Most structural and functional studies to date have been performed on the A-class oxidases, which includes those that are found in the inner mitochondrial membrane and bacteria such as *Rhodobacter sphaeroides* and *Paracoccus denitrificans* (aa_3-type oxidases in these bacteria). These oxidases pump protons with a stoichiometry of one proton per electron transferred to the catalytic site. The bacterial A-class oxidases use two proton pathways (denoted by letters D and K, respectively), for the transfer of protons to the catalytic site, and protons that are pumped across the membrane. The B-type oxidases such as, for example, the ba_3 oxidase from *Thermus thermophilus*, pump protons with a lower stoichiometry of 0.5 H^+/electron and use only one proton pathway for the transfer of all protons. This pathway overlaps in space with the K pathway in the A class oxidases without showing any sequence homology though. Here, we review the functional properties of the A- and the B-class ba_3 oxidases with a focus on mechanisms of proton transfer and pumping. This article is part of a Special Issue entitled: Respiratory Oxidases.

1. Introduction

The last component of the respiratory chains in many bacteria, archaea and in mitochondria is a membrane-bound heme-copper oxidase, which catalyzes the reduction of O_2 to H_2O. For cytochrome *c* oxidases (CytcOs), the electron donor is reduced cytochrome *c*, i.e. the overall reaction catalyzed by these enzymes is:

$$4c^{2+} + 4H^+ + O_2 \rightarrow 4c^{3+} + 2H_2O \quad (1)$$

The free energy available from oxidation of cytochrome c^{2+} and reduction of O_2 is determined by the midpoint potentials of cytochrome c^{2+}/c^{3+} (the electron donor) and the O_2/H_2O couple (the electron acceptor). At pH 7, 25° C and 1 atm O_2 the difference between these potentials is ~500 mV. This difference is relatively insensitive to the O_2 concentration because four electrons are required for reduction of one O_2 molecule to water. Thus, for a factor of 10 decrease in O_2 concentration the redox-potential difference decreases by approx. 60 mV/4 = 15 mV.

The catalytic site where O_2 is reduced consists of a heme group and a copper site situated in close vicinity (typically at a distance of ~5 Å) and a Tyr residue (see below) [1–11]. The O_2-reduction reaction in heme-copper oxidases is arranged in space such that the electrons and protons are supplied from different sides of the membrane. The electrons are donated from the more positive side (*p* side), whereas protons are taken up from the more negative (*n* side) of the membrane (for a review of the general features of this reaction, see [12–17]). Consequently, the reaction results in a charge separation across the membrane. Assuming a transmembrane proton electrochemical gradient equivalent to ~200 mV, this charge separation results in conservation of about ~40% (200 mV/540 mV, see above) of the free energy available from O_2 reduction. In addition, the heme-copper oxidases studied to date have been shown to conserve free energy by pumping protons from the *n* to the *p* side across the membrane, thereby increasing the fraction of conserved energy to ~$(40+\eta\,40)$%, where η is the number of protons translocated across the membrane for each electron transferred to O_2. The overall reaction catalyzed by the oxidases can be summarized as:

$$4e_p^- + 4(1+\eta)H_n^+ + O_2 \rightarrow 2H_2O + 4\eta H_p^+ \quad (2)$$

where the subscripts refer to the two sides of the membrane. The free energy that is stored in the electrochemical gradient is used e.g. for transmembrane transport processes and ATP production.

The heme-copper catalytic site is buried within the membrane-spanning part of the enzyme at a distance of ~25 Å and ~15 Å from the *n*-side and *p*-side surface, respectively. Consequently, specific proton-conducting pathways are needed for transfer of protons from solution to the catalytic site. Furthermore, a proton pathway

☆ This article is part of a Special Issue entitled: Respiratory Oxidases.

* Corresponding author. Tel.: +46 8 163280; fax: +46 8 153679.
E-mail address: peterb@dbb.su.se (P. Brzezinski).

0005-2728/$ – see front matter © 2012 Elsevier B.V. All rights reserved.
doi:10.1016/j.bbabio.2011.11.015

across the entire membrane thickness (~40 Å) must be provided to transfer protons that are pumped across the membrane. This latter pathway must be "gated" such that protons are taken up from the *n*-side (lower proton concentration) and delivered to the *p*-side (higher proton concentration). The gate may consist, for example, of a protonatable amino-acid residue that would switch between two conformations with proton connectivities to either the *n*- or *p*-side of the membrane, but never to both sides simultaneously. In addition, the pK_a of this group may change from a high to a low value when in contact with the *n*- or *p*-sides of the membrane, respectively (but this is not a necessary requirement, [18]). In this context, variants of the term proton-loading site (PLS) have been used to describe a site, which temporarily binds protons that are to be pumped across the membrane, but not those delivered to the catalytic site. The PLS itself may be a gate, or it may be located in close proximity to other structural components involved in proton gating.

Proton pathways in proteins are typically composed of water molecules coordinated by amino-acid residues, as well as polar and charged amino-acid side chains. Inspection of X-ray crystal structures of heme-copper oxidases, together with genomic analyses have identified a number of oxidase classes with a different number and composition of the proton-conducting pathways. In this review, we focus on two such classes, denoted by letters A and B (for this particular type of classification, see [19,20]).

2. Electron transfer and proton pathways in the A and B-class oxidases

2.1. A-class

The A-class includes the mitochondrial cytochrome *c* oxidase (Cyt*c*O), which consists of 13 subunits [7]. The three core subunits of this enzyme are highly homologous to the corresponding subunits in many bacterial oxidases, including the well-studied aa_3 (letter denote the type of hemes in these enzymes, see below) oxidases from *Rhodobacter sphaeroides* and *Paracoccus denitrificans* (Fig. 1ab) [21]. High-resolution structures have been obtained of these two bacterial Cyt*c*Os [5,6,9] as well as of the mitochondrial Cyt*c*O from bovine heart [7]. In these enzymes electrons are donated by a water-soluble cytochrome *c*, which docks to the enzyme at the *p* side of the membrane, and delivers electrons, one at a time, to a copper site called Cu_A. From here, electrons are transferred over a distance of 19.4 Å (Cu_A to the heme iron) to heme *a* and then to the catalytic site, which consists of heme a_3 and Cu_B, approximately parallel to the membrane surface. The distance between the heme *a* and a_3 iron ions is 13.5 Å and that between the heme a_3 iron and Cu_B is 4.8 Å (PDB ID: 1M56, [6]). All the A-class Cyt*c*Os studied to date pump protons with a stoichiometry of one proton per electron transferred to the catalytic site, i.e. η in Eq. (2) equals to one leading to an energy conservation of 80% [13,16,22,23].

In the bacterial A-class oxidases, protons are transferred through two conserved proton pathways [24,25]. One of these pathways is denoted by the letter K and starts near $Glu101^{II}$ (all residues in A-class oxidases are numbered according to the *R. sphaeroides* cytochrome aa_3 sequence and the superscript indicates the subunit number, where no superscript indicates subunit I) [26]. The pathway leads via a water molecule that is hydrogen-bonded to Ser299, to the highly conserved Lys362 residue after which the pathway is named. This residue is connected, via another water molecule and Thr359 to Tyr288 at the catalytic site (Fig. 1c). The second pathway, denoted by the letter D after a highly-conserved and functionally important Asp132 residue near the orifice of the pathway, leads via about 10 intraprotein water molecules to another conserved acidic residue, Glu286. The pathway is lined by a number of polar residues, many of which are highly conserved.

The K pathway is used for uptake of two protons upon transfer of two electrons to the catalytic site, i.e. one electron to heme a_3 and one to Cu_B [24,27,28] see also [29]. This two-electron reduction of the catalytic site allows binding of O_2 to heme a_3 and, after initiation of the O_2 reduction, the remaining two protons needed for water formation (see Eq. (1)) are transferred through the D pathway. The D pathway is also used for transfer of all four protons that are pumped across the membrane, which means that a total of six protons are transferred through this pathway for each O_2 reduced to H_2O. In other words, during reduction of the catalytic site, the two substrate protons are transferred through the K pathway, while the two pumped protons are transferred through the D pathway. In the steps subsequent to O_2 binding, both the two substrate protons and the two pumped protons are transferred through the D pathway (Fig. 1c). The mechanistic asymmetry in the distribution of the number of protons between the D and K pathways in different parts of the reaction cycle is not fully understood. Both pathways connect the *n*-side surface with the catalytic site. Yet, after O_2 binding, the K pathway is not used for proton transfer and this is true even if the D pathway is blocked by a mutation(s) [30,31].

In the mitochondrial Cyt*c*O, a third so called H-pathway has been suggested to be used exclusively for transfer of the pumped protons. This pathway has been shown not to be operational in the bacterial A-class oxidases and it is not discussed in detail here. For further reading on the structure and function of the H-pathway we refer to [32].

2.2. B-class

One representative member of the B-class oxidases is cytochrome ba_3 from *Thermus thermophilus*. Several X-ray crystal structures of this enzyme have been determined at atomic resolution [1–4] (Fig. 1de).

The kinetics of electron and proton transfer during reaction of the reduced ba_3 Cyt*c*O with O_2 have recently been investigated in more detail [33–38]. In this enzyme, upon reduction, the sequence of electron transfers is the same as described above for the A-class oxidases, except that heme *a* is replaced by heme *b*, i.e. the sequence is cytochrome *c* → Cu_A → heme *b* → heme a_3/Cu_B (Fig. 1f). The distances between the metal sites are very similar to those found in the A-class oxidases; Cu_A — heme *a*, 19.2 Å; heme *b* — heme a_3, 13.9 Å; heme a_3 — Cu_B, 4.4 Å (between metal centers) (PDB ID: 1XME, [39]). The *T. thermophilus* ba_3 Cyt*c*O pumps protons, but with a stoichiometry of 0.5 proton per electron transferred to the catalytic site, i.e. η in Eq. (2) is 0.5 and the overall energy conservation is ~60% [40,41]. The lower pumping stoichiometry is not due to the low O_2 concentrations at which the *T. thermophilus* lives, ~10 μM O_2 [2,42]. Even at such low O_2 concentrations, the electron donor–acceptor redox potential difference would be decreased by only ~30 mV compared to a saturated O_2 solution (~1.2 mM at 1 atm, 25 C), leaving sufficiently free energy for pumping of one proton per electron transferred to O_2.

An early inspection of the X-ray crystal structure of this enzyme suggested the presence of three putative proton pathways [1]. However, surprisingly, results from later functional studies indicated that only one proton pathway is operational in the ba_3 Cyt*c*O [3]. This pathway overlaps in space with the K pathway in the A-class oxidases and it is therefore referred to as a "K-pathway analog", without sharing any structural similarity with aa_3 K-channel though (c.f. Fig. 1c and f).

In the following, we discuss results from kinetic studies of the reaction of the reduced *R. sphaeroides* aa_3 and *T. thermophilus* ba_3 Cyt*c*Os with O_2 with a specific emphasis on reaction steps that involve proton transfer to the catalytic site and proton pumping. The experimental approach involves first reduction of all four metal sites, i.e. by four electrons (This state is denoted $\mathbf{R^2}$, where the superscript indicates the number of electrons residing at the catalytic site — heme a_3 and Cu_B each reduced by one electron. In addition, there are two electrons at Cu_A and heme *a*, i.e. the Cyt*c*O is reduced by a total of four electrons). The specific sub steps associated with the reaction

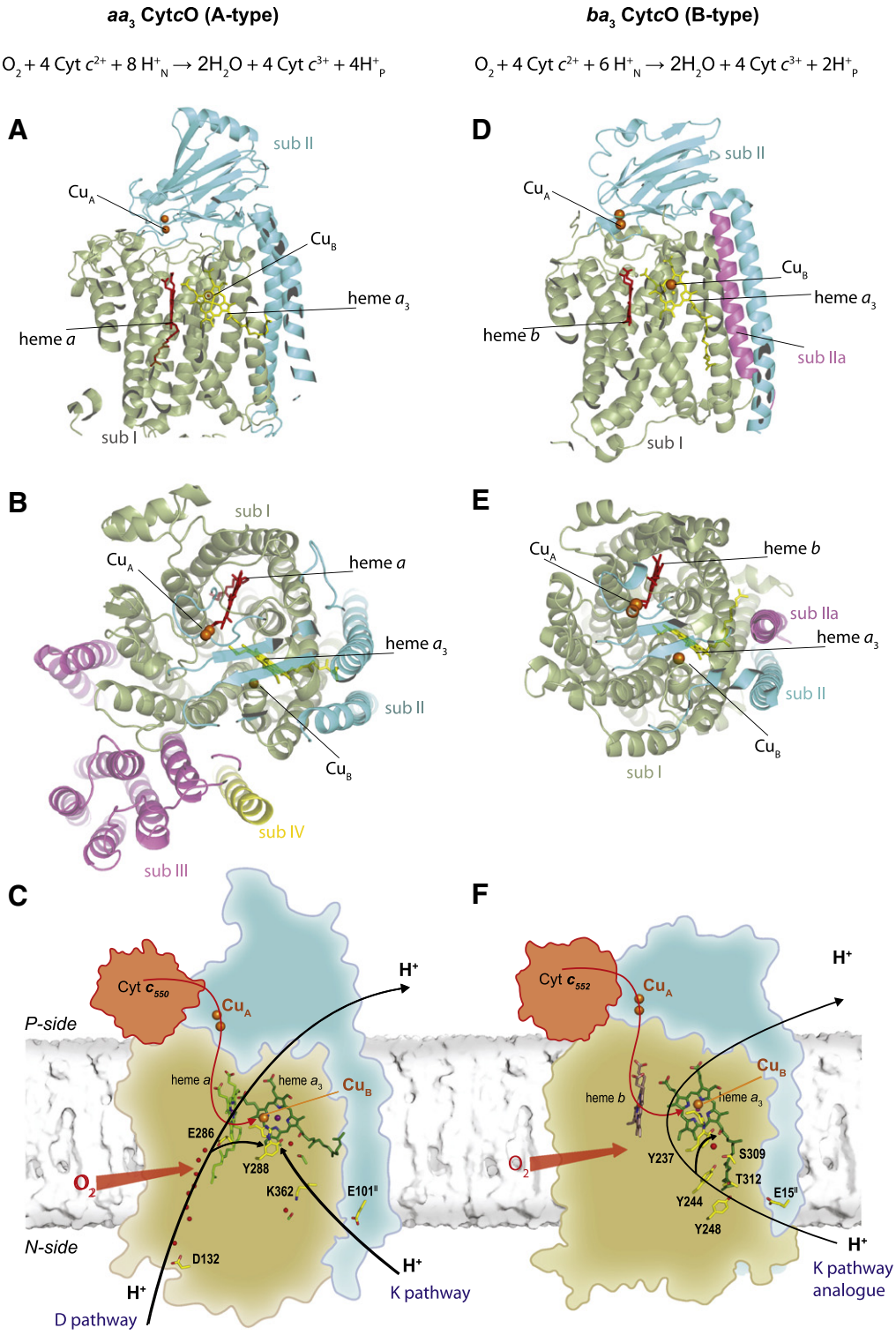

Fig. 1. Structures of the A-class *Rhodobacter sphaeroides* aa_3 CytcO (PDB ID: 1M56) (A–C) and the B-class *Thermus thermophilus* ba_3 CytcO (PDB ID: 1XME) (D–F). These enzymes consist of four and three subunits (sub), respectively, as indicated in different colors. In the aa_3 CytcO, subunit IV consists of only one transmembrane helix of unknown function. The sub II transmembrane helices in the *R. sphaeroides* CytcO correspond to those of subs II and IIa in the *T. thermophilus* CytcO. Metal sites heme *a*/*b*, heme a_3 and Cu_B are all found in sub I. Cu_A is found in sub II. In the ba_3 CytcO sub I consists of 13 helices, i.e. one more than in the corresponding subunit of the *R. sphaeroides* CytcO. The 13th helix does not superimpose with any of the transmembrane helices of the A-class oxidases with known structures. Panels (C) and (F) show schematic views of the aa_3 and ba_3 CytcOs, respectively, with amino-acid residues and water molecules (red spheres) defining the proton pathways. In both CytcOs, electrons are transferred from cytochrome *c* to Cu_A, heme *a*/*b* to the catalytic site (red arrow). Oxygen enters the catalytic site through a channel located in the membrane-spanning part of the protein as indicated by the bold arrow. Protons are transferred along the black arrows. The reactions catalyzed the aa_3 and ba_3 CytcOs are shown in the upper part of the figure, where the former and latter pump 4 and 2 protons, respectively, for each O_2 that is reduced. Panels a,b,d and e were prepared using the program PyMOL [55].

of the four-electron reduced Cyt*c*O and O_2 cannot be observed just by mixing the Cyt*c*O and O_2 because the electron and proton-transfer reactions occur over time scales in the microsecond domain. To circumvent this problem, the blocking ligand carbon monoxide is introduced into the sample containing the reduced Cyt*c*O, which results in binding of CO to heme a_3 at the catalytic site and thereby blocking the access of O_2. The CO–Cyt*c*O complex is mixed with a solution containing O_2 after which the CO ligand is dissociated using a short laser flash. This approach, referred to as the "flow-flash technique", bypasses the problem associated with mixing and allows the synchronized binding of O_2 to the catalytic site such that the reaction can be followed in time with an adequate time resolution.

3. Reaction of the A-class oxidases with O_2

The reaction sequences of the A-class *P. denitrificans* and mitochondrial Cyt*c*Os are very similar to that observed with the *R. sphaeroides* Cyt*c*O and in the following we focus on the latter enzyme. The results from kinetic studies have been summarized in a number of other review papers such as, for example, [13,14,16,17,43,44]. Here, we give a brief summary that is used as a basis for the comparison of these reactions with those observed in the B-class ba_3 oxidase. In the *R. sphaeroides* aa_3 Cyt*c*O, after CO dissociation, O_2 binds to heme a_3 with a time constant of ~10 μs at 1 mM O_2 (state $\mathbf{A^2}$, here the superscript "2" indicates the number of electrons added to the oxidized catalytic site, one to heme a_3 and one to Cu_B) (Fig. 3a). This reaction is followed in time by electron transfer from heme *a* to the catalytic site and breaking of the O-O bond with a time constant of ~30 μs. In this process, a proton is transferred from Tyr 288 in the catalytic site to the reduced O_2 molecule. The state that is formed is called "peroxy" or $\mathbf{P_R}$. Here, we call this state $\mathbf{P^3}$ to indicate that 3 electrons are transferred to the catalytic site upon its formation. An intermediate state with the same chemical structure is also formed upon addition of only two electrons to the catalytic site (state $\mathbf{P_M}$), where an additional electron required for the O – O bond breaking is taken from Tyr 288, which forms an amino-acid radical. Here, the $\mathbf{P_M}$ state is denoted $\mathbf{P^2}$ to indicate the number of electrons transferred to the catalytic site (see Fig. 2 and discussion below, Tyr 288 is considered being part of the catalytic site).

Until formation of $\mathbf{P^3}$, there is no proton uptake from solution or proton pumping. In the next step though, a proton is taken up from solution through the D pathway to the catalytic site forming the "ferryl" state **F**, here denoted $\mathbf{F^3}$, with a time constant of ~100 μs at pH 7.5. The $\mathbf{P^3 \rightarrow F^3}$ reaction is also linked in time to pumping of a proton (the proton is taken up via the D pathway) across the membrane and electron transfer from Cu_A to heme *a*, which results in ~50% reduction of the heme. It should be noted that the $\mathbf{P^3 \rightarrow F^3}$ reaction does not involve any electron transfer to the catalytic site and that the proton-transfer reactions (both to the catalytic site and proton pumping) are triggered only by formation of state $\mathbf{P^3}$ and are independent of the electron transfer from Cu_A to heme *a* [45]. A proton is taken up to the catalytic site and a proton is pumped across the membrane even if the electron remains at Cu_A (this situation can be created and studied in a mutant Cyt*c*O in which the Cu_A midpoint potential is dramatically increased) [23].

In the last step of the reaction, the electron in the Cu_A/heme *a* equilibrium is transferred to the catalytic site, linked to proton uptake from solution through the D pathway, forming the oxidized state **O**, here denoted $\mathbf{O^4}$, with a time constant of ~1 ms (at pH ~7). The $\mathbf{F^3 \rightarrow O^4}$ reaction is also linked in time to pumping of a proton across the membrane (also via the D pathway).

We note that formation of the $\mathbf{P^3}$ state involves rapid electron transfer from heme *a* to the catalytic site (see Fig. 3). This is the case because in the experiments outlined above, the reaction is initiated with Cyt*c*O that is fully reduced prior to O_2 binding and heme *a* is reduced at the time of O_2 binding. Because the electron transfer from heme *a* to the catalytic site is faster than proton uptake, the two processes can be separated in time such that $\mathbf{A^2 \rightarrow P^3}$ involves only electron transfer, while $\mathbf{P^3 \rightarrow F^3}$ involves only proton transfer to the catalytic site. During turnover, when electrons are transferred to the catalytic site from an external donor (i.e. significantly slower), during O – O bond breaking an electron is taken from Tyr288 in the catalytic site. The state that is formed is chemically equivalent to $\mathbf{P^3}$, but its formation involves only local electron re-distribution within the catalytic site and therefore it carries one less negative charge, i.e. it is denoted $\mathbf{P^2}$. As with $\mathbf{P^3}$, up to this point in the reaction there is no proton uptake from solution. The next step, $\mathbf{P^2 \rightarrow F^3}$, involves simultaneous electron and proton transfer to the catalytic site. In other words, during turnover (or even when electrons are added one-by-one from an external donor to the catalytic site) it is not possible to separate in time electron transfer from proton transfer. The final step in the reaction of the fully reduced Cyt*c*O with O_2, $\mathbf{F^3 \rightarrow O^4}$, involves simultaneous electron and proton transfer to the catalytic site, which means that this reaction is representative of the situation during turnover of the Cyt*c*O.

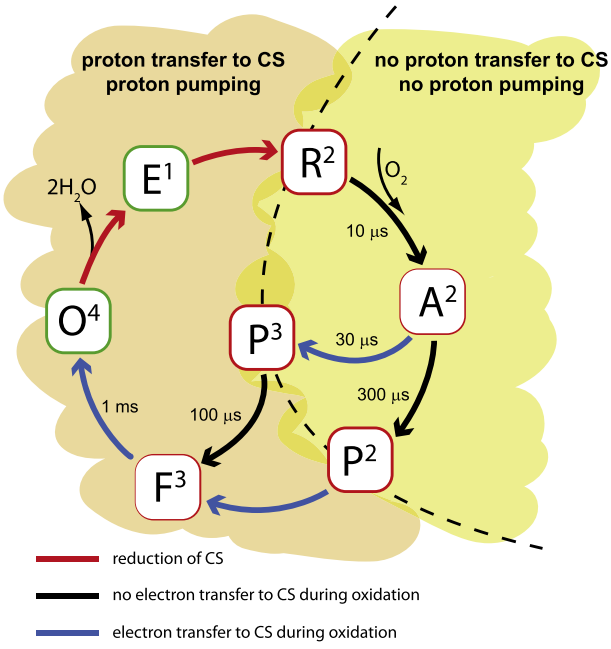

Fig. 2. A schematic reaction cycle of the A-class oxidases. The different states of the Cyt*c*O are indicated by the one-letter codes, where the superscript indicates the number of electrons transferred to the catalytic site. Here $\mathbf{P^2}$ and $\mathbf{P^3}$ are equivalent to $\mathbf{P_M}$ and $\mathbf{P_R}$, respectively. Reduction of the oxidized Cyt*c*O (state $\mathbf{O^4}$, equivalent to $\mathbf{O^0}$) results in consecutive reduction of the catalytic site (CS) by one ($\mathbf{E^1}$) and two ($\mathbf{R^2}$) electrons. These reactions are linked in time to proton uptake to the catalytic site and proton pumping. Note that the superscript only reflects the number of electrons at the catalytic site, but not on the other two sites. In $\mathbf{R^2}$ there are two electrons at the catalytic site, while the other two sites, Cu_A and heme *a*, may or may not be reduced. In the fully reduced Cyt*c*O each of these sites is reduced by one electron (i.e. the Cyt*c*O is reduced by a total of four electrons). Upon formation of $\mathbf{R^2}$, O_2 binds to heme a_3. During turnover, when electrons are transferred from cytochrome *c* via Cu_A and heme *a* to the catalytic site, this binding is followed in time by splitting of the O – O bond and formation of the peroxy ($\mathbf{P^2}$) state. The other reaction pathway via $\mathbf{P^3}$ is used only when starting with the fully reduced Cyt*c*O, while the pathway via $\mathbf{P^2}$ is used when electrons are added one-by-one from cytochrome *c* to the Cyt*c*O. This is because in the fully reduced Cyt*c*O, heme *a* is reduced upon O_2 binding and the initial O_2-reduction step involves also electron transfer from heme *a* to the catalytic site (c.f. $\mathbf{P^3}$ has one more electron at the catalytic site than $\mathbf{P^2}$). Both $\mathbf{P^3 \rightarrow F^3}$ and $\mathbf{P^2 \rightarrow F^3}$ reactions involve proton transfer to the catalytic site and proton pumping across the membrane, while the $\mathbf{P^2 \rightarrow F^3}$ reaction additionally involves electron transfer to the catalytic site. The $\mathbf{F^3 \rightarrow O^4}$ reaction involves electron and proton transfer to the catalytic site as well as proton pumping. In summary, for the overall cycle, in the case of the reaction of the fully reduced with O_2, the four required electrons are added to the oxidized Cyt*c*O already upon forming $\mathbf{R^2}$ and the pathway via $\mathbf{P^3}$ is used. During "normal" turnover, reduction of the oxidized Cyt*c*O involves first reduction by only two electrons and then two additional electrons are transferred to the Cyt*c*O during the $\mathbf{P^2 \rightarrow F^3}$ and $\mathbf{F^3 \rightarrow O^4}$ steps.

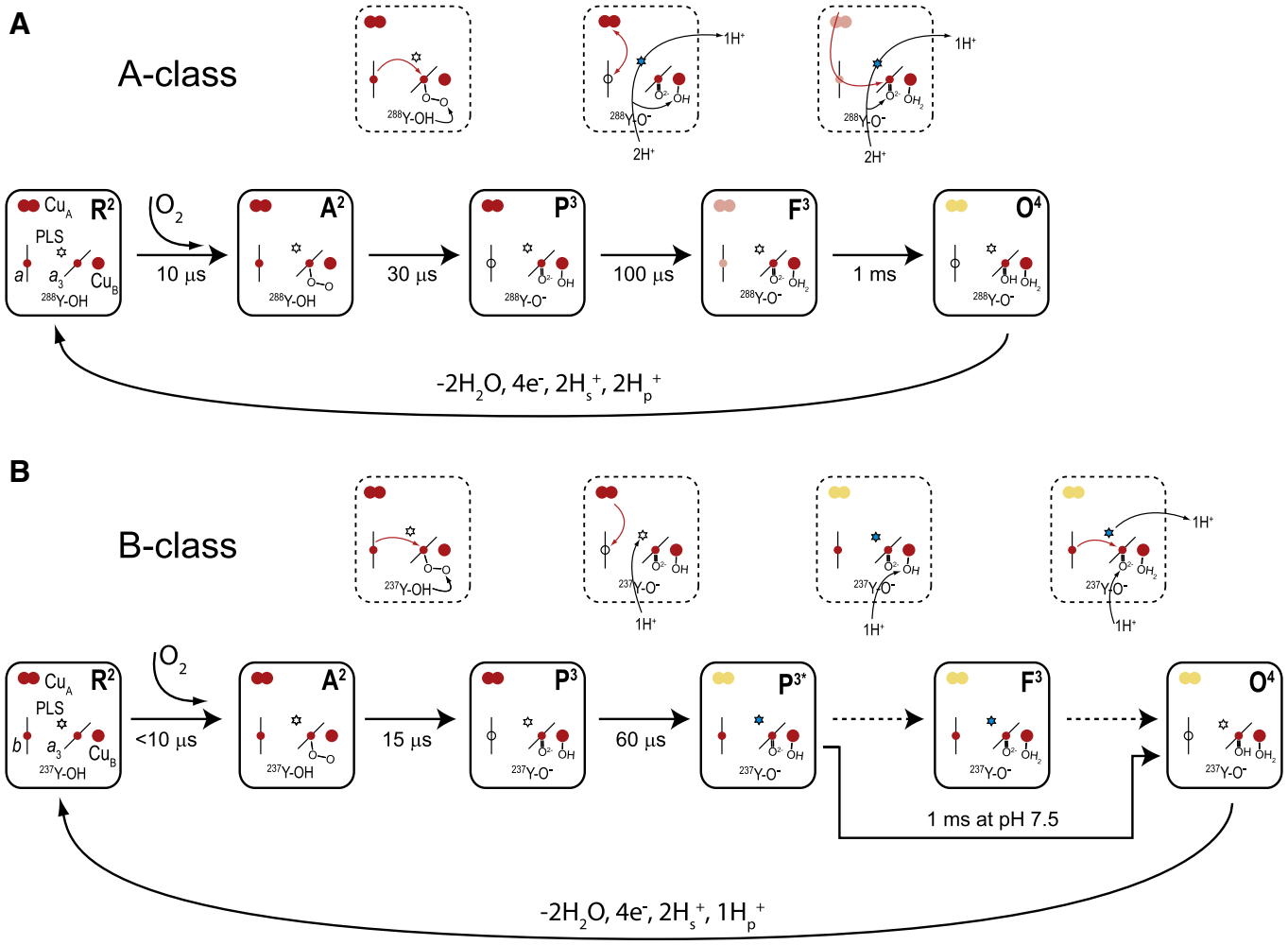

Fig. 3. The reaction of the reduced aa_3 (A) and ba_3 (B) Cyt*c*O with O_2. The reaction is also described in the legend to Fig. 2. In addition to the metal sites, here also Tyr288 (Y–OH) is shown. PLS is the "proton-loading site". The dashed boxes indicate the reaction that takes place in the different steps. The lower arrow indicates that for the A-class oxidases, during reduction of the oxidized state ($\mathbf{O^4}$) two water molecules are released, four electrons are transferred to the Cyt*c*O, two substrate protons are taken up and two protons are taken up and released at the other side of the membrane. The same $\mathbf{O^4 \rightarrow R^2}$ reaction takes place for the B-class oxidase, except that only one proton is pumped. In the ba_3 oxidase, the $\mathbf{F^3}$ state is not observed because it is formed and decays over the same time scale at neutral pH; only one kinetic phase corresponding to the $\mathbf{P^3 \rightarrow O^4}$ reaction is observed.

Another important point is the timing of proton-transfer reactions during the $\mathbf{P^3 \rightarrow F^3}$ and $\mathbf{F^3 \rightarrow O^4}$ reaction steps as seen using the flow-flash approach. These reaction steps involve proton uptake to the catalytic site as well as the uptake and release of protons that are pumped across the membrane. Knowing the exact order of these reactions is important for understanding the mechanism. However, even though the time resolution of the experiments would allow observation of each of these proton-transfer events, in every of the reaction steps ($\mathbf{P^3 \rightarrow F^3}$ and $\mathbf{F^3 \rightarrow O^4}$), all proton-transfer events occur as a single kinetic phase ($\tau \cong 100$ µs and $\tau \cong 1$ ms at pH ~7, respectively) [23,46], meaning that for each reaction the rate-limiting step is the same.

3.1. pH dependence

During reaction of the reduced Cyt*c*O with O_2, the reactions until formation of state $\mathbf{P^3}$ display a very weak pH dependence, consistent with the absence of proton uptake from solution up to formation of $\mathbf{P^3}$. On the other hand, the rates of both reaction steps that follow in time after $\mathbf{P^3}$, $\mathbf{P^3 \rightarrow F^3}$ and $\mathbf{F^3 \rightarrow O^4}$, display significant pH dependencies. The $\mathbf{P^3 \rightarrow F^3}$ rate is pH independent at low pH (~10^4 s^{-1}) and then decreases at higher pH values. A pK_a value of 9.4 was extracted from this pH dependence and this pK_a was attributed to titration of Glu286 [47], which is an internal proton donor/acceptor within the D pathway. Recently, an alternative explanation for this pH dependence was presented [48], where Asp132 that is located close to the protein surface, was proposed to titrate with a pK_a of 9.4. We find this alternative explanation to be unlikely in part based on the location of this residue in a relatively hydrophilic environment.

The $\mathbf{F^3 \rightarrow O^4}$ reaction titrates with two pK_a values of ~9 and <6.4 [49,50]. Because this reaction involves the same proton-transfer events as the $\mathbf{P^3 \rightarrow F^3}$ reaction, we have previously attributed the higher pK_a to a titration of Glu286. The lower pK_a on the other hand, reflects the protonation state of groups near heme *a*, which influences electron transfer to the catalytic site (this titration is absent for the $\mathbf{P^3 \rightarrow F^3}$ reaction because it is not linked to electron transfer to the catalytic site) [49].

4. Reaction of the B-class oxidases with O_2

After dissociation of CO from the four-electron reduced ba_3 Cyt*c*O, O_2 binds with a time constant of ~5 µs [36] forming state $\mathbf{A^2}$. Electron transfer from heme *b* to the catalytic site is faster than with the A-class CytcOs and the $\mathbf{P^3}$ state is formed with a time constant of ~15 µs at neutral pH [35–37] (Fig. 3b). As with A-class oxidases, formation of $\mathbf{P^3}$ is followed in time by proton uptake from solution and electron transfer from Cu_A to heme *b*. This reaction displays a time

constant of ~60 μs at neutral pH, which is slightly faster than with the A-class CytcOs (~100 μs). In the ba_3 CytcO, the Cu_A to heme *b* electron transfer results in nearly 100% heme *b* reduction, which means that the equilibrium is shifted more towards the heme in the ba_3 than in e.g. the *R. sphaeroides* A-class CytcO (c.f. [36] and [44]). However, the main difference between the ba_3 and A-class CytcOs is that in the ba_3 CytcO the $\mathbf{F^3}$ state is not formed upon proton uptake ($\tau \cong 60$ μs) from solution. This means that the proton is presumably not transferred to the catalytic site to form $\mathbf{F^3}$, but rather to another protonatable group located at a distance from the catalytic site [36,38]. Based on results from a recent study, we speculated that this site is a loading site for protons that are pumped across the membrane (see below) [38].

From here on, the scenario is more complicated for the ba_3 oxidase than with the A-class oxidases. Therefore, we first discuss the reaction of the three-electron reduced ba_3 CytcO with O_2, i.e. in this case there is no additional electron transfer to the catalytic site after the reaction steps outlined above. Up to $\mathbf{P^3}$ formation and the 60-μs proton uptake, the reaction is essentially identical to that described above (except a slightly slower proton uptake, $\tau \cong 70$ μs instead of 60 μs), but in this case it is possible to observe events that follow in time after formation of $\mathbf{P^3}$ without interference from internal transfer of the fourth electron. The data showed that there is a significant difference between this reaction in the B-type oxidase and the corresponding reaction observed for the A-class oxidases. In the latter case, upon transfer of three electrons to the catalytic site, proton uptake occurs in only one kinetic phase with a time constant of ~100 μs (a net of one proton is taken up and one proton is pumped across the membrane, i.e. simultaneously taken up and released, also at $\tau \cong 100$ μs). However, with the ba_3 oxidase, after the initial 70-μs proton uptake, there is an *additional* proton-uptake reaction with a time constant of ~1 ms at neutral pH that is linked in time to formation of state $\mathbf{F^3}$. Thus, with the ba_3 CytcO, transfer of three electrons to the catalytic site triggers proton uptake in *two* kinetic phases, where the first proton ($\tau \cong 70$ μs) is taken up to a site located at a distance from the catalytic site (suggested to be the PLS), while the second proton ($\tau \cong 1$ ms) is transferred to the catalytic site to form $\mathbf{F^3}$ (Figs. 3b and 4b).

Upon reaction of the four-electron reduced ba_3 CytcO with O_2, transfer of the last electron from heme *b* to form the oxidized CytcO occurs with a time constant of 0.9 ms at neutral pH and this reaction is linked in time to proton uptake from solution. We note that the time constant of the final oxidation step is about the same as that for formation of $\mathbf{F^3}$ as outlined above, explaining why with the ba_3 CytcO state $\mathbf{F^3}$ is not populated to any significant degree during reaction of the four-electron reduced CytcO and O_2 [36,38]. Thus, the observed reaction sequence with the ba_3 CytcO is $\mathbf{A^2 \rightarrow P^3 \rightarrow O^4}$.

The question that arises is, at which step(s) are the pumped protons taken up and released in the ba_3 CytcO? Based on the data with the three-electron reduced CytcO [38], and earlier electrometric measurements [36], over the time scale of the first proton uptake ($\tau \cong 60$ μs) there is presumably no proton pumping. We suggested earlier that this is the reaction step at which the loading site for pumped protons, the PLS, becomes protonated [38]. Based on the data with the three-electron reduced CytcO, another proton is then transferred to the catalytic site with a time constant of ~1 ms to form $\mathbf{F^3}$. Because a net proton uptake is observed, there is presumably no release of a pumped proton, linked to $\mathbf{F^3}$ formation. When four electrons are available within the CytcO at pH 7.5, this proton uptake coincides in time with electron transfer to the catalytic site to form $\mathbf{O^4}$, but the net amount of protons taken up upon formation of $\mathbf{F^3}$ (in the three-electron reduced CytcO) and upon formation of $\mathbf{O^4}$ (in the four-electron reduced CytcO) is approximately the same. This is surprising because in the A-class oxidases, one more proton is taken up upon formation of $\mathbf{O^4}$ compared to $\mathbf{F^3}$. Furthermore, it is known that the $\mathbf{F^3 \rightarrow O^4}$ reaction requires uptake of a proton to the catalytic site and, therefore, we would expect the net proton uptake to be larger for the reaction of the four-electron than for the three-electron reduced ba_3 CytcOs. One plausible explanation to account for this "missing proton" was discussed in [38] where we suggested that during formation of state $\mathbf{O^4}$ the "60-μs proton" loaded at PLS is released. To summarize, upon reaction of the four-electron reduced ba_3 CytcO with O_2, one proton is taken up to the PLS after $\mathbf{P^3}$ formation with a time constant of ~60 μs, then formation of $\mathbf{F^3}$ is linked to an additional proton uptake. The subsequent $\mathbf{F^3 \rightarrow O^4}$ reaction is linked to the uptake of one more proton along with the simultaneous proton release from the PLS (at pH 7.5). Because the time constants of $\mathbf{F^3}$ formation and the $\mathbf{F^3 \rightarrow O^4}$ reaction are approximately the same, the *net* proton-uptake stoichiometry is apparently the same independently of whether the reaction stops at $\mathbf{F^3}$ or $\mathbf{O^4}$.

4.1. pH dependence

With the ba_3 CytcO, the formation rate of state $\mathbf{P^3}$ is essentially pH-independent. The rate of the first proton uptake, linked to electron transfer from Cu_A to heme *b* is also essentially pH-independent in the pH range 5–10. A very small pH dependence is observed for formation of the $\mathbf{F^3}$ state and the associated proton-uptake reaction; the time constant increases from ~0.5 ms at pH 5 to ~2 ms at pH 10. The last reaction step, i.e. formation of the oxidized CytcO ($\mathbf{O^4}$) is the only reaction that displays a significant pH dependence of the rate; the time constant increases from ~0.7 ms at pH 5.5 to ~20 ms at pH 11 [38].

The absence of any pH dependence for the formation rate of $\mathbf{P^3}$ is consistent with observations with the A-class oxidases and the fact that there is no proton uptake or release during this reaction [44,51]. However, for the following reaction steps, the pH-dependence of the reactions in the A- class and ba_3 oxidases differ significantly. In the former case, the $\mathbf{P^3 \rightarrow F^3}$ reaction rate is pH-dependent and displays a Henderson–Hasselbalch titration with a pK_a of 9.4, where the pK_a is attributed to titration of the Glu286 residue [47]. As already mentioned above, the $\mathbf{F^3 \rightarrow O^4}$ reaction also displays a significant pH dependence where the main titration is observed in two pH regions, $pK_{a1} \cong 9$, attributed to titration of Glu286, and $pK_{a2} < 6$, attributed to titration of groups near the hemes [49,50].

The absence of any pH dependence for the rate of proton uptake to the PLS or to the catalytic site (to form $\mathbf{F^3}$) in the ba_3 CytcO can be explained in terms of involvement of protonatable group(s) having pK_a(s) outside of the measured pH range. For example, even though with the A-class *R. sphaeroides* CytcO the $\mathbf{P^3 \rightarrow F^3}$ reaction displays a titration with a pK_a of 9.4, some single-site mutations in the pathway result in an elevation of this pK_a such that the proton-uptake rate becomes pH-independent in the experimentally available pH range [52,53].

5. Comparison of the reactions in A- and B-class oxidases

Fig. 4a summarizes a reaction scheme of the A-type CytcO turnover (c.f. for example [17]). During the $\mathbf{F^3 \rightarrow O^4}$ reaction, which is comparable to a typical reaction step during turnover (*i*) an electron is transferred to the catalytic site, (*ii*) a pumped proton is taken up from the *n* side of the membrane to the PLS, (*iii*) a substrate proton is transferred from the *n* side to the catalytic site and (*iv*) the proton at PLS is released to the *p* side solution. Under most conditions, these partial reactions cannot be time-resolved and appear to occur simultaneously. Also in the special case when an electron is transferred very rapidly to the catalytic site prior to proton uptake (upon $\mathbf{P^3}$ formation as outlined above), the proton-transfer reactions (*ii*)–(*iv*) in the $\mathbf{P^3 \rightarrow F^3}$ reaction all display the same time constant.

The situation is distinctly different in the B-CytcO. After (*i*) electron transfer to the catalytic site to form $\mathbf{P^3}$, a proton is taken up and suggested to be transferred to the PLS from the *n*-side of the membrane with $\tau \cong 60$ μs (*ii*), then another proton is transferred

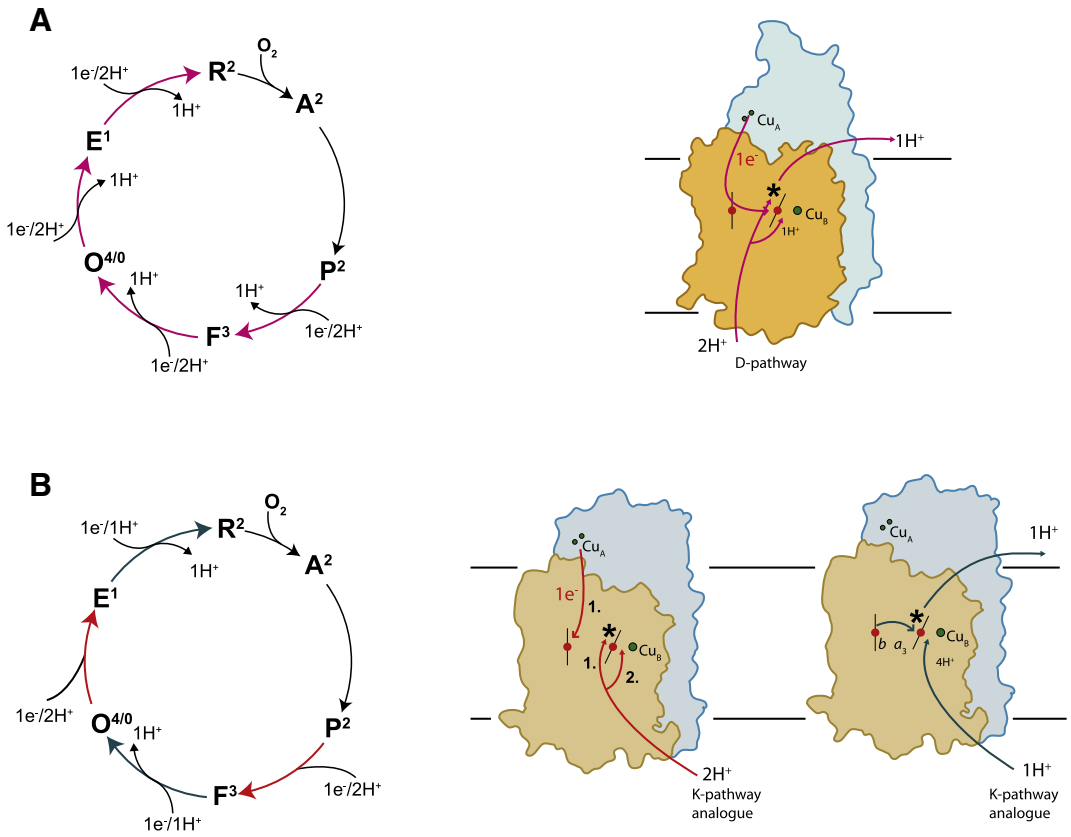

Fig. 4. A model showing the sequence of electron and proton-transfer reactions in the A-type (A) and B-type (B) oxidases. (A) In the A-class oxidases electron transfer to the catalytic site is linked in time to proton uptake to the catalytic site as well as proton uptake to PLS (*) and release from PLS (proton that is pumped across the membrane). This sequence of events occurs for the reaction steps indicated in the color magenta on the left-hand side. Note that during $O^0 \rightarrow E^1 \rightarrow R^2$ substrate protons are taken up through the K pathway. (B) We propose that in the B-class oxidases for every second electron transfer to the catalytic site a proton is either taken up or released from the PLS (*) (see corresponding arrow colors on the right- and left-hand sides of panel B). The experimental data suggest that a "pumped proton" is released during $F^3 \rightarrow O^4$ [36,38], which would imply that the next step ($O^0 \rightarrow E^1$) is linked to proton uptake to PLS, while $E^1 \rightarrow R^2$ is linked to proton release. The step preceding $F^3 \rightarrow O^4$, i.e. $P^2 \rightarrow F^3$ must then also be linked to proton uptake to the PLS.

from the *n*-side to the catalytic site to form state $\mathbf{F^3}$ with $\tau \cong 1$ ms (*iii*). There is no proton release from PLS to the *p*-side (*iv*) until transfer of the next electron to the catalytic site to form $\mathbf{O^4}$. The two proton-uptake reactions (*ii*) and (*iii*) are observed as separate events in the reaction of the fully reduced ba_3 CytcO with O_2 because electron transfer to the catalytic site (reaction (*i*)) is much faster than these proton-uptake events.

Based on these results from studies of the reaction of reduced ba_3 CytcO with O_2, we speculate that during turnover, for every electron transfer to the catalytic site a proton would either be taken up or released to/from PLS (Fig. 4b) [38].

This scenario would explain the observed 0.5 H^+/electron pumping stoichiometry in the B-CytcOs [40,41]. According to this suggested scenario, the lower stoichiometry is not due to pumping of 0.5 H^+ in each step, but rather due to pumping of 1 H^+ in every second step. Furthermore, it should be noted that the 50% lower pumping stoichiometry in the ba_3 CytcO does not mean that the energy-conservation efficiency is 50% of that of the A-class CytcOs. This is because also the O_2-reduction reaction catalyzed by the CytcOs in itself leads to a charge separation across the membrane (see Introduction). Consequently, the total charge translocation stoichiometry for the A-class and ba_3 CytcOs is 2 and 1.5, respectively, charges transferred across the membrane per electron transferred to the catalytic site.

Since only one proton pathway is used in the ba_3 CytcO, gating at two levels is required. First, the pumped protons must be gated as outlined above to prevent proton leaks across the membrane. Second, the transfer of substrate and pumped protons through the K-pathway analog must be controlled in order to assure that the free energy available from O_2 reduction is conserved. The data discussed above indicate that in the ba_3 oxidase this is accomplished by transfer of a proton to the PLS before a proton is transferred to the catalytic site. This separation in time of the two events would assure that the PLS is protonated before the reaction at the catalytic site proceeds. In a recent paper, Gennis and colleagues argued that the absence of a D pathway in the ba_3 CytcO is related to the high O_2 affinity of the B-class oxidases [41]. Briefly, the O_2 channels in CytcOs overlap in space with the D pathway. In the A-class oxidases, Glu286, at the end of the D pathway, is presumably involved in controlling the timing of proton transfer to the catalytic site and the PLS [54]. Because the ba_3 CytcO harbors a particularly large O_2 channel [1,2] that is decorated by hydrophobic residues, the presence of such a channel excludes proton transfer through this region of the protein [41]. The K pathway analog in the ba_3 CytcO leads to the catalytic site and control of the order of proton transfer events to the catalytic site and PLS may require a more distinct time separation of these events as compared to the A-class CytcOs in which substrate and pumped protons are separated in space at a site (Glu286) located at a distance from the catalytic site.

The discovery of the alternating sequence of electron transfer and loading and unloading of the PLS in the cytochrome ba_3 oxidases offers an exciting opportunity to gain functional insights into the CytcO pumping machinery in future studies of mutant forms of the ba_3 CytcO.

Abbreviations and definitions

CytcO, cytochrome *c* oxidase. *n*, *p*-side, negative and positive sides of the membrane, respectively. Intermediate states that appear during turnover the CytcO (the superscript indicates the number of electrons added to the oxidized catalytic site): $\mathbf{R^2}$, reduced catalytic site (one electron added to each of heme a_3 and Cu_B); $\mathbf{A^2}$, O_2 bound to

heme a_3 at the reduced catalytic site; $\mathbf{P^2}$, (also called $\mathbf{P_M}$) "peroxy" state formed upon reaction of the two-electron reduced catalytic site with O_2; $\mathbf{P^3}$, (also called $\mathbf{P_R}$) "peroxy" state formed upon reaction of O2 with the reduced catalytic site, where an electron is transferred from heme *a* to the catalytic site simultaneously with the O_2 reduction; $\mathbf{F^3}$, "ferryl" state at the catalytic site; $\mathbf{O^4}$, oxidized catalytic site (equivalent to $\mathbf{O^0}$). Time constants are given as (rate constant)$^{-1}$. If not otherwise indicated, amino-acid residues are numbered according to the *Rhodobacter sphaeroides* Cyt*c*O sequence.

Acknowledgements

Part of the studies described in this review was supported by grants from the Swedish Research Council (to PB and PÄ), and by grant HL 16101 from the National Institutes of Health (to RBG.). CvB is supported by a fellowship from the Swiss National Science Foundation (SNF). PÄ is a Royal Swedish Academy of Sciences Research Fellow supported by a grant from the Knut and Alice Wallenberg Foundation.

References

[1] T. Soulimane, G. Buse, G.P. Bourenkov, H.D. Bartunik, R. Huber, M.E. Than, EMBO J. 19 (2000) 1766–1776.
[2] V.M. Luna, Y. Chen, J.A. Fee, C.D. Stout, Biochemistry 47 (2008) 4657–4665.
[3] H.Y. Chang, J. Hemp, Y. Chen, J.A. Fee, R.B. Gennis, Proc. Natl. Acad. Sci. U. S. A. 106 (2009) 16169–16173.
[4] T. Tiefenbrunn, W. Liu, Y. Chen, V. Katritch, C.D. Stout, J.A. Fee, V. Cherezov, High resolution structure of the ba_3 cytochrome *c* oxidase from *Thermus thermophilus* in a lipidic environment. PLoS One. 6 (7) (2011).
[5] S. Iwata, C. Ostermeier, B. Ludwig, H. Michel, Nature 376 (1995) 660–669.
[6] M. Svensson-Ek, J. Abramson, G. Larsson, S. Törnroth, P. Brzezinski, S. Iwata, J. Mol. Biol. 321 (2002) 329–339.
[7] T. Tsukihara, H. Aoyama, E. Yamashita, T. Tomizaki, H. Yamaguchi, K. Shinzawa-Itoh, R. Nakashima, R. Yaono, S. Yoshikawa, Science 272 (1996) 1136–1144.
[8] J. Liu, L. Qin, S. Ferguson-Miller, Proc. Natl. Acad. Sci. U. S. A. 108 (2011) 1284–1289.
[9] L. Qin, C. Hiser, A. Mulichak, R.M. Garavito, S. Ferguson-Miller, Proc. Natl. Acad. Sci. U. S. A. 103 (2006) 16117–16122.
[10] K. Shinzawa-Itoh, H. Aoyama, K. Muramoto, H. Terada, T. Kurauchi, Y. Tadehara, A. Yamasaki, T. Sugimura, S. Kurono, K. Tsujimoto, T. Mizushima, E. Yamashita, T. Tsukihara, S. Yoshikawa, EMBO J. 26 (2007) 1713–1725.
[11] H. Aoyama, K. Muramoto, K. Shinzawa-Itoh, K. Hirata, E. Yamashita, T. Tsukihara, T. Ogura, S. Yoshikawa, Proc. Natl. Acad. Sci. U. S. A. 106 (2009) 2165–2169.
[12] J.P. Hosler, S. Ferguson-Miller, D.A. Mills, Annu. Rev. Biochem. 75 (2006) 165–187.
[13] I. Belevich, M.I. Verkhovsky, Antioxid. Redox Signal. 10 (2008) 1–29.
[14] S. Ferguson-Miller, G.T. Babcock, Chem. Rev. 96 (1996) 2889–2907.
[15] M. Wikström, M.I. Verkhovsky, Biochim. Biophys. Acta (BBA), Bioenerg. 1767 (2007) 1200–1214.
[16] P. Brzezinski, R.B. Gennis, J. Bioenerg. Biomembr. 40 (2008) 521–531.
[17] V.R.I. Kaila, M.I. Verkhovsky, M. Wikström, Chem. Rev. 110 (2010) 7062–7081.
[18] B.G. Malmström, Biochim. Biophys. Acta 811 (1985) 1–12.
[19] M.M. Pereira, M. Santana, M. Teixeira, Biochim. Biophys. Acta, Bioenerg. 1505 (2001) 185–208.
[20] J. Hemp, R.B. Gennis, Results Probl. Cell Differ. 45 (2008) 1–31.
[21] J.P. Hosler, J. Fetter, M.M. Tecklenburg, M. Espe, C. Lerma, S. Ferguson-Miller, J. Biol. Chem. 267 (1992) 24264–24272.
[22] D. Bloch, I. Belevich, A. Jasaitis, C. Ribacka, A. Puustinen, M.I. Verkhovsky, M. Wikström, Proc. Natl. Acad. Sci. U. S. A. 101 (2004) 529–533.
[23] K. Faxén, G. Gilderson, P. Ädelroth, P. Brzezinski, Nature 437 (2005) 286–289.
[24] A.A. Konstantinov, S. Siletsky, D. Mitchell, A. Kaulen, R.B. Gennis, Proc. Natl. Acad. Sci. U. S. A. 94 (1997) 9085–9090.
[25] J.R. Fetter, J. Qian, J. Shapleigh, J.W. Thomas, A. García-Horsman, E. Schmidt, J. Hosler, G.T. Babcock, R.B. Gennis, S. Ferguson-Miller, Proc. Natl. Acad. Sci. U. S. A. 92 (1995) 1604–1608.
[26] M. Brändén, F. Tomson, R.B. Gennis, P. Brzezinski, Biochemistry 41 (2002) 10794–10798.
[27] K. Ganesan, R.B. Gennis, Biochim. Biophys. Acta, Bioenerg. 1797 (2010) 619–624.
[28] M. Brändén, H. Sigurdson, A. Namslauer, R.B. Gennis, P. Ädelroth, P. Brzezinski, Proc. Natl. Acad. Sci. U. S. A. 98 (2001) 5013–5018.
[29] M. Wikström, A. Jasaitis, C. Backgren, A. Puustinen, M.I. Verkhovsky, Biochim. Biophys. Acta 1459 (2000) 514–520.
[30] I.A. Smirnova, P. Ädelroth, R.B. Gennis, P. Brzezinski, Biochemistry 38 (1999) 6826–6833.
[31] L. Salomonsson, G. Brändén, P. Brzezinski, Biochim. Biophys. Acta, Bioenerg. 1777 (2008) 343–350.
[32] K. Shimokata, Y. Katayama, H. Murayama, M. Suematsu, T. Tsukihara, K. Muramoto, H. Aoyama, S. Yoshikawa, H. Shimada, Proc. Natl. Acad. Sci. U. S. A. 104 (2007) 4200–4205.
[33] A. Giuffrè, E. Forte, G. Antonini, E. D'Itri, M. Brunori, T. Soulimane, G. Buse, Biochemistry 38 (1999) 1057–1065.
[34] S. Siletskiy, T. Soulimane, N. Azarkina, T.V. Vygodina, G. Buse, A. Kaulen, A. Konstantinov, FEBS Lett. 457 (1999) 98–102.
[35] I.A. Smirnova, D. Zaslavsky, J.A. Fee, R.B. Gennis, P. Brzezinski, J. Bioenerg. Biomembr. (2008) 1–7.
[36] S.A. Siletsky, I. Belevich, A. Jasaitis, A.A. Konstantinov, M. Wikström, T. Soulimane, M.I. Verkhovsky, Biochim. Biophys. Acta 1767 (2007) 1383–1392.
[37] I. Smirnova, J. Reimann, C. Von Ballmoos, H.Y. Chang, R.B. Gennis, J.A. Fee, P. Brzezinski, P. Ädelroth, Biochemistry 49 (2010) 7033–7039.
[38] C. Von Ballmoos, R.B. Gennis, P. Ädelroth, P. Brzezinski, Proc. Natl. Acad. Sci. U. S. A. 108 (2011) 11057–11062.
[39] L.M. Hunsicker-Wang, R.L. Pacoma, Y. Chen, J.A. Fee, C.D. Stout, Acta Crystallogr. D: Biol. Crystallogr. 61 (2005) 340–343.
[40] A. Kannt, T. Soulimane, G. Buse, A. Becker, E. Bamberg, H. Michel, FEBS Lett. 434 (1998) 17–22.
[41] H. Han, J. Hemp, L.A. Pace, H. Ouyang, K. Ganesan, J.H. Roh, F. Daldal, S.R. Blanke, R.B. Gennis, Proc. Natl. Acad. Sci. 108 (2011) 14109–14114.
[42] B.H. Zimmermann, C.I. Nitsche, J.A. Fee, F. Rusnak, E. Munck, Proc. Natl. Acad. Sci. U. S. A. 85 (1988) 5779–5783.
[43] Ó. Einarsdóttir, I. Szundi, Biochim. Biophys. Acta, Bioenerg. 1655 (2004) 263–273.
[44] P. Ädelroth, M. Ek, P. Brzezinski, Biochim. Biophys. Acta 1367 (1998) 107–117.
[45] M. Karpefors, P. Ädelroth, Y. Zhen, S. Ferguson-Miller, P. Brzezinski, Proc. Natl. Acad. Sci. U. S. A. 95 (1998) 13606–13611.
[46] A. Jasaitis, M.I. Verkhovsky, J.E. Morgan, M.L. Verkhovskaya, M. Wikström, Biochemistry 38 (1999) 2697–2706.
[47] A. Namslauer, A. Aagaard, A. Katsonouri, P. Brzezinski, Biochemistry 42 (2003) 1488–1498.
[48] M. Wikström, M.I. Verkhovsky, Biochim. Biophys. Acta 1807 (10) (2011) 1273–1278.
[49] G. Brändén, M. Brändén, B. Schmidt, D.A. Mills, S. Ferguson-Miller, P. Brzezinski, Biochemistry 44 (2005) 10466–10474.
[50] A. Namslauer, P. Brzezinski, FEBS Lett. 567 (2004) 103–110.
[51] S. Hallén, T. Nilsson, Biochemistry 31 (1992) (1859) 11853–11859.
[52] P. Brzezinski, A.L. Johansson, Biochim. Biophys. Acta, Bioenerg. 1797 (2010) 710–723.
[53] A.L. Johansson, S. Chakrabarty, C.L. Berthold, M. Högbom, A. Warshel, P. Brzezinski, Biochim. Biophys. Acta 1807 (9) (2011) 1083–1094.
[54] V.R.I. Kaila, M.I. Verkhovsky, G. Hummer, M. Wikström, Biochim. Biophys. Acta, Bioenerg. 1787 (2009) 1205–1214.
[55] W.L. DeLano, DeLano Scientific, Palo Alto, CA, USA, 2002.